Resonant photoemission of TiN films

G. G. Fuentes, P. Prieto, C. Morant, C. Quirós, R. Núñez, L. Soriano, E. Elizalde, and J. M. Sanz*
Departamento de Física Aplicada C-XII and Instituto Universitario ''Nicolás Cabrera,'' Universidad Autónoma de Madrid, Cantoblanco E-28049 Madrid, Spain

(Received 12 April 2000; published 24 January 2001)

The bonding and electronic structure of TiN thin films grown by sputtering have been characterized by means of resonant photoemission spectroscopy using synchrotron radiation. Specifically we found a complex resonance profile that exhibits a maximum at 45 eV followed by a second structure at 50 eV. The intensity enhancement observed at 45 and 50 eV is consistent with the resonant photoemission of the Ti $3d$ states involved in the valence band of TiN and the multiplet configuration of the $[\mathrm{Ti}\,3p^5 3d^2]^*$ excited states. The autoionizing character of the $[\mathrm{Ti}\,3p^5 3d^2]^*$ states could also be confirmed by observation of the corresponding autoionization emission. The resonance is used to determine the Ti $3d$ contribution to the valence band. The results are in good agreement with calculated Ti $3d$ partial density of states.

DOI: 10.1103/PhysRevB.63.075403 PACS number(s): 79.60.−i, 71.20.−b

I. INTRODUCTION

The electronic structure of titanium nitride TiN along with other transition-metal nitrides and carbides is of considerable interest from both a technological and fundamental point of view. In fact, there are a considerable number of studies on TiN using different electron and x-ray spectroscopies,[1–20] e.g., x-ray photoemission spectroscopy (XPS), photoemission spectroscopy (PES), x-ray emission spectroscopy (XES), electron energy-loss spectroscopy (EELS), and x-ray absorption spectroscopy (XAS), as well as several theoretical studies using different approaches.[21–29] Many of these studies have paid attention to the electronic structure of substoichiometric TiN and the influence of nitrogen vacancies on its properties.[1–3,6,11]

In general, the band-structure calculations show that the bonding in these compounds is mostly covalent due to the filling of the Ti $3d-\mathrm{N}\,2p$ bonding states. The Fermi level intersects the Ti $3d$ bands, predicting a high density of states at the Fermi energy with almost pure Ti $3d$ character.[21–30]

Resonant photoemission electron spectroscopy (RPES) has been extensively used to isolate the cationic contribution to the valence band of complex hybridized compounds.[19,20,30–43] Nevertheless, and although RPES is a well-established technique, studies of the resonant phenomenon itself are also of interest since the detailed explanation of some resonance profiles recently published, e.g., TiO_2 (Refs. 36–38), ZrO_2 (Ref. 39), MoS_2 (Ref. 41), SnO (Ref. 42), and even TiN (Refs. 19, 20, and 30) remains to be given.

In the case of TiN, the pioneering work of Bringans and Höchst[19] in polycrystalline TiN_x and ZrN_x showed the existence of a rather complex dependence of the valence-band intensity on the photon energy. However, the experimental conditions did not enable a detailed analysis of the data. Didziulis *et al.*[20] have performed an RPES study on TiC(100) including some results on TiN(100) for comparison. These authors observed for both TiC and TiN an intense resonance at around 45 eV associated with the Ti $3p\rightarrow 3d$ transition as well as a much weaker resonant enhancement at 70 eV for TiC, which was labeled as due to Ti $3s\rightarrow 4p$ transitions with a question mark. More recently, Walker *et al.*[30] published a RPES study of TiN thin films deposited by magnetron sputtering. These authors observed a complex resonance profile with local maxima at 45, 48, and 73 eV. Whereas the resonance at 45 eV is interpreted as due to Ti $3p\rightarrow 3d$ excitations, the other features remain unexplained. Clearly we are far from an understanding of the RPES profiles of TiN and hence far from understanding the electronic structure and bonding of this material.

In this paper we describe details of RPES, Auger electron spectroscopy (AES), and EELS experiments on the Ti $3p\rightarrow 3d$ excitation and deexcitation processes in TiN, aimed at obtaining a better understanding of the resonance and consequently of its valence-band (VB) structure.

II. EXPERIMENT

TiN films (150 nm thick) were obtained in a dual-ion-beam sputtering system at a base pressure of 10^{-5} Pa. A Kaufmann-type ion source was used to sputter a Ti target with Ar^+ ions of 800 eV. A second ion source is then used to bombard the growing film with reactive $N_2{}^+$ ions of very low energy ($\sim$50 eV). After growth, the films are exposed to the atmosphere, causing a small contamination of oxygen that is easily removed after annealing at 800 °C for several minutes. Small amounts of carbon introduced during the deposition process ($<$5 at. %) could not be eliminated.

AES and EELS data were obtained in the integral $N(E)$ mode in a PHI-3027 spectrometer equipped with a double-pass cylindrical mirror analyzer (DPCMA). For EELS and AES we have used a primary electron energy of 500 eV. Whereas the EEL spectra were obtained with a pass energy of $\Delta E = 20$ eV, the AES spectra were measured with a constant relative energy resolution $\Delta E/E = 0.25\%$. XPS measurements confirmed that the Ti to N atomic ratio was 1. Furthermore, XPS showed that the film was oxygen-free, whereas some graphitic carbon (i.e., C $1s$ peak at 284.8 eV) was discernible at the surface of the film.

The PES experiments were performed on station 6.2 of the Daresbury Synchrotron radiation source, using photon

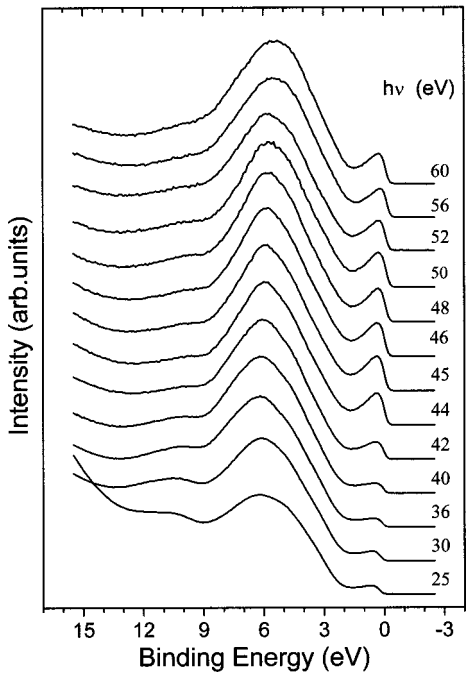

FIG. 1. Valence-band photoemission spectra of TiN as a function of the photon energy, $25<h\nu<60$ eV. The spectra have been normalized to the respective areas.

energies between 25 and 60 eV. The photoemission spectra were measured using two different grating monochromators for photon energies ranging between $15<h\nu<50$ and $50<h\nu<60$ eV, respectively. The photoemission spectra were recorded with a DPCMA at a pass energy of 15 eV that corresponds to an energy resolution of 0.2 eV. The residual pressure was better than 10^{-7} Pa. A tungsten grid was used to measure the photon flux at the entrance of the analysis chamber. The background of secondary electrons was subtracted using the Shirley method.[44] As compared with XPS, PES indicates higher carbon contamination (i.e., ~10%) due to its higher surface sensitivity. In any case, the presence of that graphitic carbon does not affect the resonant photoemission phenomenon of TiN, as will be shown later.

III. RESULTS

Figure 1 presents the energy distribution curves (EDC's) of the valence band of TiN measured at different photon energies in the range $25\leqslant h\nu\leqslant 60$ eV as labeled, after normalization to the respective total area. Figure 1 provides evidence of a significant intensity modulation of the two main features of the valence band when the photon energy is changed between 40 and 50 eV. Although the resonance manifests itself over the whole valence band, the most striking changes occur in the feature at the Fermi level, which shows a clear enhancement at photon energies above 40 eV.

Resonant photoemission of the Ti $3d$ states in TiN has been previously observed at 45 eV,[19,20,30] i.e., at photon energies above the Ti $3p\rightarrow 3d$ transition. According to the fundamentals of the phenomenon, the excitation of a Ti $3p\rightarrow 3d$ transition creates an excited state $[\mathrm{Ti}\ 3p^5 3d^2]^*$,

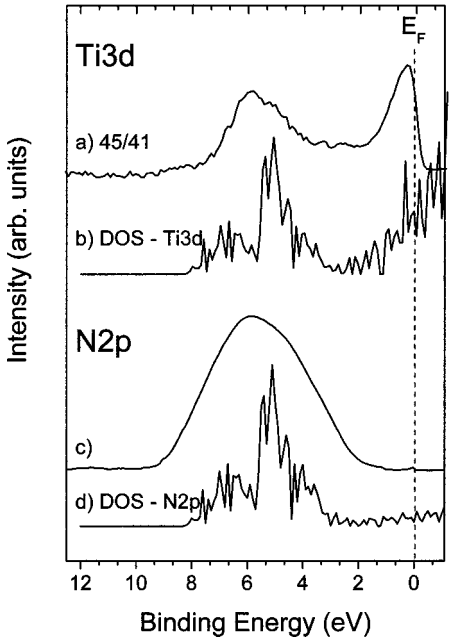

FIG. 2. Curve (a): Ti $3d$ contribution to the valence band as derived from the resonance at $h\nu=45$ eV, i.e., 45-41 difference spectrum calculated by subtracting the spectrum measured at 41 eV from that measured at 45 eV. Curve (b): Calculated Ti $3d$ density of states (cf. Ref. 18). Curve (c): N $2p$ contribution to the valence band of TiN as determined from the valence band spectrum at $h\nu=41$ eV after subtraction of a properly scaled curve (a) (see text for details). Curve (d): Calculated N $2p$ density of states (cf. Ref. 18).

which remains localized on the cation site. The excited state relaxes via a direct recombination that involves the Ti $3d$ states in the valence band and leads to the same final state as in conventional photoemission of the Ti $3d$ electrons. The interference between both processes gives rise to the resonant enhancement of those parts of the spectrum with a significant Ti $3d$ character. Since the intensity enhancement is due to an increase of the photoemission cross section of the Ti $3d$ states, it is meaningful to compute difference spectra by subtracting the EDC measured at a photon energy ''off resonance'' from that measured ''on resonance'' to isolate the cationic contribution (i.e., Ti $3d$) to the valence band. Figure 2 shows the result of subtracting the spectrum measured at 41 eV from that measured at 45 eV (cf. Fig. 1), indicating those parts of the valence band in which there is a significant contribution of Ti $3d$ states. The result is labeled as 45-41 and appears compared with the calculated Ti partial density of states (PDOS).[18] The good agreement existing between the 45-41 difference spectrum and the calculated Ti PDOS clearly supports the above interpretation according to the fundamentals of RPES.

Furthermore, the subtraction of a properly scaled 45-41 difference spectrum, as representative of the Ti contribution, from a valence-band spectrum ''off resonance'' allows to estimate the N $2p$ component of the valence band if we neglect the small Ti $4sp$–derived states. The method is equivalent to fitting the valence band at 41 eV in terms of two components, i.e., N $2p$ and Ti $3d$, weighted according to the respective photoemission cross sections.[45] The result

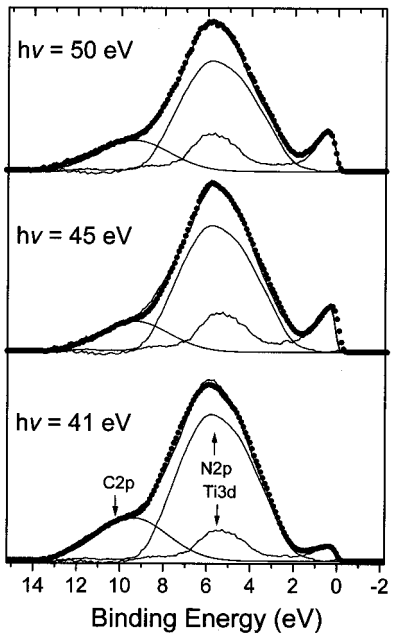

FIG. 3. Analysis of the valence-band photoemission spectra at $h\nu=50$, 45, and 41 eV using three components that correspond to Ti $3d$, N $2p$, and C $2p$ (contamination).

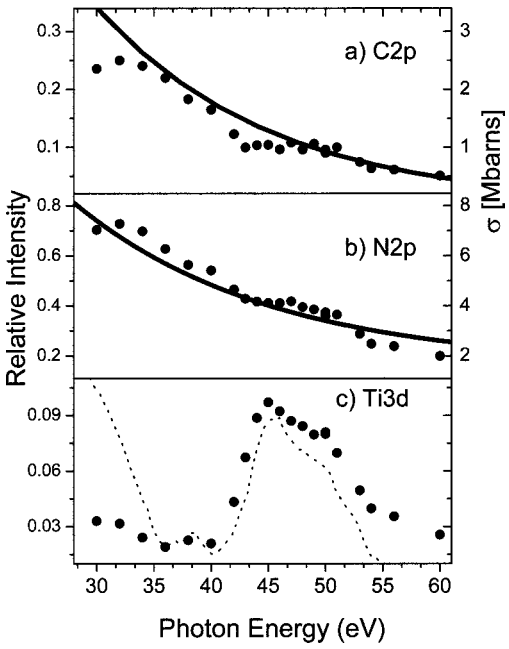

FIG. 4. Photon energy dependence ($30<h\nu<60$ eV) of the integrated intensity (points) of the (a) C $2p$, (b) N $2p$, and (c) Ti $3d$ components of the valence-band emission. The continuous lines correspond to the respective photoemission cross sections as given in Ref. 45. The dotted line is the CIS curve for the states at a binding energy of 0.5 eV measured in Ref. 30.

of this analysis has been labeled as N $2p$ in Fig. 2 [curve (c)]. For comparison, the calculated N $2p$ density of states[18] has also been depicted. The agreement is rather good and gives confidence to the procedure.

In order to get a more quantitative insight of the resonance, all the valence-band spectra have been analyzed in terms of those two main components, i.e., Ti $3d$ and N $2p$. Actually, to reproduce the whole series of spectra we had to include an extra C $2p$ band at 10.5 eV to account for the carbon contamination of the samples. In order to obtain information about the distribution profile of the different components we have used factor analysis[46,47] (FA). This is a well-established multivariate statistical method for data handling and spectral interpretation when the measured spectra can be attained by linear combination of independent individual components. In general, the main advantage of FA is that it provides an automatic procedure to establish the number and concentration of the independent components of a set of spectra. Factor analysis of the whole set of valence-band spectra depicted in Fig. 1 including the basis spectra confirms the requirement of three principal components whose shape is in very good agreement with the proposed basis, i.e., Ti $3d$, N $2p$, and C $2p$ and also allows the quantitative determination of the respective contribution as a function of the photon energy. Typical fits are shown in Fig. 3 for valence-band spectra measured at $h\nu=41$, 45, and 50 eV.

Areas of the respective components in each spectrum of the experimental series were determined and plotted versus the photon energy in Fig. 4. The plots essentially represent constant initial state (CIS) curves. Usually the resonance effects are analyzed in terms of CIS spectra, where just the intensity of the valence band at a given binding energy[19,20,41] or the intensity of arbitrary Gaussian peaks used to fit the valence band[20,32–35,41] is analyzed as a function of the photon energy. In both cases the CIS curves are of mixed character due to the hybridization of different levels, which contribute to different parts of the valence band. However, our previous analysis allows a better interpretation of the resonance profiles as the components are expected to represent states with a definite character. In the last case the CIS curves are a straightforward representation of the dependence of the respective photoemission cross section on the photon energy.

Both the C $2p$ and N $2p$ intensities decrease with increasing photon energy in good agreement with the respective theoretical atomic subshell photoionization cross sections as indicated by the continuous line included in Figs. 4(a) and 4(b). In fact, the values given on the right y scale of Fig. 4 correspond to the respective photoionization cross sections as calculated by Yeh and Lindau.[45] Additionally, the integrated intensity of the Ti $3d$ band shows a characteristic two-peak structure at energies between 45 and 50 eV with a clear intensity enhancement (i.e., approximately a factor of 3), which corresponds to the resonance process of the Ti $3d$ states. For comparison we have included a dotted line [i.e., Fig. 4(c)], showing the CIS curve for the states at 0.5 eV binding energy, which are of pure d character, as measured recently by Walker *et al.*[30] for stoichiometric TiN. It is worth noting here the general good agreement observed among these resonances in shape, energy position, and enhancement factor, which strongly supports our interpretation. Nevertheless, these authors were unable to explain the second resonance at 50 eV, suggesting that it is due to the generation of a $M_{23}M_{45}M_{45}$ Auger electron although no evidence of that Auger feature is observed in their experiments. However, we

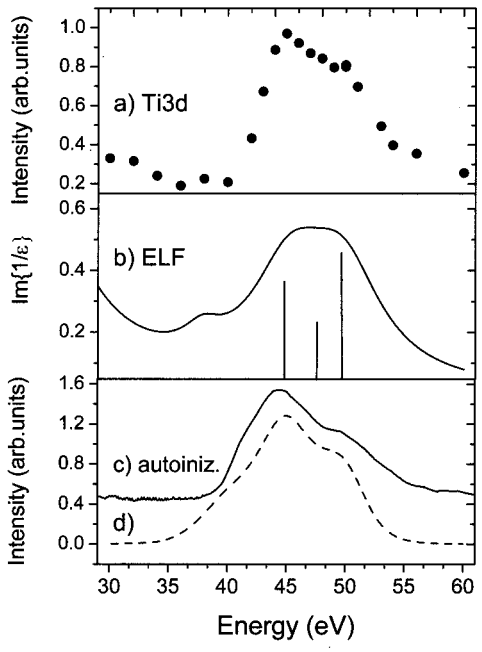

FIG. 5. Curve (a): Photon energy dependence ($30<h\nu<60$ eV) of the integrated intensity of the Ti $3d$ contribution to the valence band of TiN across the Ti $3p$ excitation threshold. Curve (b): Energy-loss function in the 30–60 eV loss energy range as determined from EELS data of Ref. 13. Vertical lines indicate the positions and relative intensities of the calculated multiplets for the Ti $3p^5 3d^2$ final state in Ti^{3+} (cf. Ref. 48). Curve (c): Measured autoionization emission (cf. Fig. 6). Curve (d): Autoionization emission calculated by convolution of the multiplet configuration of the Ti $3p^5 3d^2$ states (cf. vertical bars) with the Ti $3d$ contribution to the valence band [cf. curve (c) in Fig. 4].

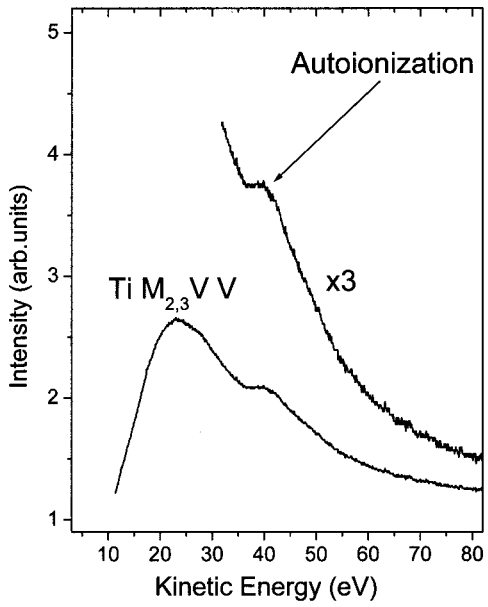

FIG. 6. Experimental $N(E)$ low-energy electron emission of TiN.

believe that both features are induced by the same resonance process, i.e., Ti $3p \rightarrow 3d$ transitions, and due to the multiplet configuration of the $[\mathrm{Ti}\ 3p^5 3d^2]^*$ excited states.

This interpretation is clearly supported by a direct observation of Fig. 5, where the resonance profile of the Ti $3d$ states is compared with the energy-loss function of TiN (i.e., $\mathrm{Im}\{1/\varepsilon\}$), as determined by EELS,[13] in the energy range 30–60 eV. The marked resemblance between both spectra is not striking because both techniques are measuring the same transitions from Ti $3p$ to $[\mathrm{Ti}\ 3p^5 3d^2]^*$ excited states. Furthermore, in order to better interpret the measured EELS spectrum and the RPES profile, we have included vertical bars that correspond to the energy position and intensity of calculated (within an *LS* coupling scheme) $3p^6 3d^1 \rightarrow 3p^5 3d^2$ transitions for isolated Ti^{3+} cations, as given by Kurahashi, Yamamoto, and Naito.[48] The comparison between the calculated and the experimental results clearly shows that both EELS and the resonance profile are reproducing the multiplet structure of the $[\mathrm{Ti}\ 3p^5 3d^2]^*$ excited states in Ti^{3+} cations.

The delay of the onset of the resonance up to about 10 eV above the Ti $3p \rightarrow$ Ti $3d$ excitation threshold (i.e., 35 eV as measured by photoemission), is also in good correlation with other delays previously observed in Ti (14 eV),[31,40] TiO_2 (9 eV),[31,36–38] Ti_2O_3 (9.5 eV),[32] and TiC (14.2 eV),[20] and seems to be a general result in other transition metals and their compounds.[32,33,39,41] Such delays are explained in terms of interactions between the $3p$ hole and the $(n+1)$ $3d$ electrons that shifts some multiplets by several electron volts. In fact, considering the good agreement between the $3p$ transitions calculated by Kurahashi, Yamamoto, and Naito[48] and those observed experimentally, we suggest that the delay is mainly caused by the Coulomb interaction between the $3p$ hole and the $3d$ electrons, because this was the only interaction considered in the calculations.[48]

Since in TiN the $[\mathrm{Ti}\ 3p^5 3d^2]^*$ excited states are autoionizing levels that induce a strong absorption, one should also expect to see strong autoionization emissions in this material. The processes leading to autoionization emission would be as follows:

$$[3p^5 3d^2]^* \rightarrow 3p^6 3d^0 + e^-.$$

The autoionization should be observable as a satellite associated with the $M_{23}VV$ Auger transitions and should resemble the shape of the M_{23} electron energy loss and the resonant photoemission spectra. Therefore we looked for autoionization emissions at the low-kinetic-energy electron emission of TiN. The measured spectrum, excited by a primary-electron beam of 500 eV, has been presented in Fig. 6. The spectrum is in good agreement with that published by Dawson and Tzatzov[10] and is dominated by two features at energies around 24 and 40 eV, which can be interpreted as an $\mathrm{Ti}(3p)\mathrm{N}(2p)\mathrm{Ti}(3d)$ Auger transition, i.e., $M_{23}VV$, and an autoionization. The first peak at 24 eV is therefore due to the Auger emission $M_{2,3}VV$ whose kinetic energy can be estimated as $E[\mathrm{Ti}\ 3p]-E[\mathrm{N}\ 2p]-E[\mathrm{Ti}\ 3d]-\Phi$ (i.e., neglecting the Coulomb interaction of the two final holes), where $E[\mathrm{Ti}\ 3p]=35$ eV, $E[\mathrm{Ti}\ 3d]=0.5$ eV, $E[\mathrm{N}\ 2p]=5.4$ eV are the respective binding energies of the core levels involved and $\Phi=4.8$ eV is the work function of the ana-

lyzer. Using these values, we obtain 24.2 eV for the Ti($3p$)N($2p$)Ti($3d$) Auger transition, in reasonable agreement with the energy actually measured. With respect to the broad feature observed at a kinetic energy of 40.2 eV with a shoulder at 45 eV [cf. Fig. 5(c)] our interpretation is that it is due to an autoionization emission originated in the excited states $[\mathrm{Ti}\ 3p^5 3d^2]^*$. In our case, the excited states $[\mathrm{Ti}\ 3p^5 3d^2]^*$ at 45 and 50 eV above the ground state decay by a direct transfer of the energy to electrons of the conduction band. The kinetic energy E_{auto} can be easily estimated in terms of the excitation energy E_{exc} (i.e., 45 and 50 eV) and the binding energy of the Ti $3d$ band at the Fermi energy, i.e., $E_{\mathrm{auto}}=E_{\mathrm{exc}}-E[\mathrm{Ti}\ 3d]-\Phi=39.8$ and 44.8 eV. The autoionization emission is then expected at 39.8 and 44.8 eV, respectively, in very good agreement with the measured energies.

The two features of the autoionization peak can be better observed in Fig. 5(c), where the autoionization peak has been depicted after background subtraction. Furthermore, Fig. 5(c) gives clear evidence that not only the energy position, but also the line shape of the autoionization resemble very well those of the RPES profile and the EELS spectrum. For comparison the autoionization feature has been shifted in energy to take into account the differences between the Fermi energy and the vacuum level, i.e., 4.8 eV. We note that the apparent multiplet structure is observable and reflected in the autoionization emission as well. The resemblance is not surprising since the shape of the autoionization is determined by the convolution of the Ti $3d$ states with the multiplet structure of the $[\mathrm{Ti}\ 3p^5 3d^2]^*$ states, which are filled by the resonant transition preceding the autoionization. The result of this convolution (i.e., Ti $3d$ states as represented by the 45-41 difference spectrum with the multiplets calculated by Kurahashi, Yamamoto, and Naito[48] after some Gaussian broadening) is also shown in Fig. 5(d). The agreement with the measured spectrum gives confidence to the interpretation. In general, Fig. 5 gives a graphical demonstration that the different experiments, electron loss, electron excited autoionization, and resonant photoemission, all stem from the same autoionization levels associated with $\mathrm{Ti}\ 3p^6 3d^1 \rightarrow [\mathrm{Ti}\ 3p^5 3d^2]^*$ transitions.

IV. SUMMARY AND CONCLUSIONS

The electronic structure of TiN thin films grown by sputtering has been studied by means of resonant photoemission spectroscopy using synchrotron radiation. Specifically we found a resonance profile that exhibits a maximum at 45 eV followed by a second structure at 50 eV. The intensity enhancement observed at 45 and 50 eV is consistent with the resonant photoemission of the Ti $3d$ states involved in the valence band of TiN. We have shown that the double peak originates from the multiplet configuration of the $[\mathrm{Ti}\ 3p^5 3d^2]^*$ excited states in Ti^{3+} ions. These excited states have also been observed by EELS, in good agreement with the measured resonance profile. Furthermore, the autoionizing character of the $[\mathrm{Ti}\ 3p^5 3d^2]^*$ states could also be confirmed by observation of the corresponding autoionization emission. Making use of the resonance, we have experimentally determined the Ti $3d$ contribution to the valence band and showed that it is in good agreement with calculated Ti $3d$ PDOS.

ACKNOWLEDGMENTS

The authors are pleased to acknowledge the financial support of the CICYT and DGICYT of Spain through Contract Nos. MAT99-0201 and PB96-0061, respectively, and the EU-TMR program under Contract No. ERBFMGCT950055 at the SRS at CLRC Daresbury Laboratory.

*Author to whom correspondence should be addressed. Electronic address: josem.sanz@uam.es

[1] L. I. Johansson, P. M. Stefan, M. L. Shek, and A. N. Christensen, Phys. Rev. B **22**, 1032 (1980).
[2] L. I. Johansson, A. Callenås, P. M. Stefan, A. Nørlund Christensen, and K. Schwarz, Phys. Rev. B **24**, 1883 (1981).
[3] P. A. P. Lindberg, L. I. Johansson, J. B. Lindström, and D. S. L. Law, Phys. Rev. B **36**, 939 (1987).
[4] J. Pflüger, J. Fink, G. Crecelius, K. P. Bohnene, and H. Winter, Solid State Commun. **44**, 489 (1982).
[5] J. Pflüger, J. Fink, W. Weber, K. P. Bohnen, and C. Grecelius, Phys. Rev. B **30**, 1155 (1984).
[6] L. Porte, L. Roux, and J. Hanus, Phys. Rev. B **28**, 3214 (1983).
[7] G. Indlekofer, J. M. Mariot, W. Lengauer, E. Beauprez, P. Oelhafen, and C. F. Hague, Solid State Commun. **72**, 419 (1989).
[8] D. W. Fischer, J. Appl. Phys. **40**, 4151 (1969); **41**, 3922 (1970).
[9] V. A. Gubanov, E. Z. Kurmaev, and G. P. Shveikin, J. Phys. Chem. Solids **38**, 201 (1977).
[10] P. T. Dawson and K. K. Tztzov, Surf. Sci. **249**, 223 (1991).
[11] H. Höchst, R. D. Bringans, P. Steiner, and Th. Wolf, Phys. Rev. B **25**, 7183 (1982).
[12] L. Soriano, M. Abbate, H. Pen, M. T. Czyzyk, and J. C. Fuggle, J. Electron Spectrosc. Relat. Phenom. **62**, 197 (1993).
[13] G. G. Fuentes, I. G. Mancheño, F. Balbás, C. Quirós, J. F. Trigo, F. Yubero, E. Elizalde, and J. M. Sanz, Phys. Status Solidi A **175**, 429 (1999).
[14] M. Delfino, J. A. Fair, and D. Hodul, J. Appl. Phys. **71**, 6079 (1992).
[15] M. J. Vasile, A. B. Emerson, and F. A. Baiocchi, J. Vac. Sci. Technol. A **8**, 99 (1990).
[16] H. Bender, J. Portillo, and W. Vandervorst, Surf. Interface Anal. **14**, 337 (1989).
[17] A. Bendavid, P. J. Martin, R. P. Netterfield, and T. J. Kinder, Surf. Interface Anal. **24**, 627 (1996).
[18] L. Soriano, M. Abbate, H. Pen, P. Prieto, and J. M. Sanz, Solid State Commun. **102**, 291 (1997).
[19] R. D. Bringans and H. Höchst, Phys. Rev. B **30**, 5416 (1984).
[20] S. V. Didziulis, J. R. Lince, T. B. Stewart, and E. A. Eklund, Inorg. Chem. **33**, 1979 (1994).
[21] A. Neckel, P. Rastl, R. Eibler, P. Weinberger, and K. Schwarz, J. Phys. C **9**, 579 (1976).
[22] P. Marksteiner, P. Weinberger, A. Neckel, R. Zeller, and P. H. Dederichs, Phys. Rev. B **33**, 812 (1986).
[23] V. P. Zhukov, V. A. Gubanov, O. Jepsen, N. E. Christensen, and

O. K. Andersen, J. Phys. Chem. Solids **49**, 841 (1988).
[24] V. P. Zhukov, N. I. Medvedeva, and V. A. Gubanov, Phys. Status Solidi B **151**, 407 (1989).
[25] V. A. Pai, A. P. Sathe, and V. R. Marathe, J. Phys.: Condens. Matter **2**, 9363 (1990).
[26] A. L. Ivanovskii and V. A. Zhilyaev, Phys. Status Solidi B **168**, 9 (1991).
[27] A. L. Ivanovskii and G. P. Shveikin, Phys. Status Solidi B **181**, 251 (1994).
[28] L. Benco, Solid State Commun. **94**, 861 (1995).
[29] L. I. Johansson, Surf. Sci. Rep. **21**, 177 (1995).
[30] C. G. H. Walker, C. A. Anderson, A. Mckinley, N. M. D. Brown, and A. M. Joyce, Surf. Sci. **383**, 248 (1997).
[31] E. Bertel, R. Stockbauer, and T. E. Madey, Phys. Rev. B **27**, 1939 (1983).
[32] K. E. Smith and V. E. Henrich, Phys. Rev. B **38**, 9571 (1988).
[33] R. Courths, B. Cord, and H. Saalfeld, Solid State Commun. **70**, 1047 (1989).
[34] J. M. Themlin, R. Sporken, J. Darville, R. Caudano, and J. M. Gilles, Phys. Rev. B **42**, 11 914 (1990).
[35] J. R. Lynce, S. V. Didziulis, J. A. Yarmoff, Phys. Rev. B **43**, 4641 (1991).
[36] Z. Zhang, Shin-Puu Jeng, and V. E. Henrich, Phys. Rev. B **43**, 12 004 (1991).
[37] R. Heise, R. Courths, and S. Witzel, Solid State Commun. **84**, 599 (1992).
[38] J. Nerlov, Q. Ge, and P. J. Møller, Surf. Sci. **348**, 28 (1996).
[39] C. Morant, A. Fernández, A. R. González-Elipe, L. Soriano, A. Stampfl, A. M. Bradshaw, and J. M. Sanz, Phys. Rev. B **52**, 11 711 (1995).
[40] T. Kaurila, J. Väyrynen, and M. Isokallio, J. Electron Spectrosc. Relat. Phenom. **78**, 71 (1996).
[41] K. C. Prince, V. R. Dhanak, P. Finetti, J. F. Walsh, R. Davis, C. A. Muryn, H. S. Dhariwal, G. Thornton, and G. Van der Laan, Phys. Rev. B **55**, 9520 (1997).
[42] V. M. Jiménez, G. Lassaletta, A. Fernández, J. P. Espinós, F. Yubero, A. R. González-Elipe, L. Soriano, J. M. Sanz, and D. A. Papaconstantopoulos, Phys. Rev. B **60**, 11 171 (1999).
[43] L. C. Davis, J. Appl. Phys. **59**, R25 (1986).
[44] D. A. Shirley, Phys. Rev. B **5**, 4709 (1972).
[45] J. J. Yeh and I. Lindau, At. Data Nucl. Data Tables **32**, 1 (1985).
[46] E. R. Malinowski and D. G. Howery, *Factor Analysis in Chemistry* (Wiley, New York, 1980).
[47] S. Hofmann and J. Steffen, Surf. Interface Anal. **14**, 59 (1989).
[48] M. Kurahashi, M. Yamamoto, and S. Naito, J. Phys.: Condens. Matter **7**, L463 (1995).